Please cite the Published Version

RESEARCH ARTICLE

WILEY

Log D$_{7.4}$ and plasma protein binding of synthetic cannabinoid receptor agonists and a comparison of experimental and predicted lipophilicity

Andrew M. Brandon[1,2] | Steven R. Baginski[1] | Caroline Peet[3,4] | Pat Dugard[1] |
Henrik Green[5,6] | Oliver B. Sutcliffe[7] | Niamh Nic Daéid[1] |
Lorna A. Nisbet[1] | Kevin D. Read[3] | Craig McKenzie[1,8]

[1]Leverhulme Research Centre for Forensic Science, School of Science and Engineering, University of Dundee, Dundee, UK

[2]Newcastle University Centre for Cancer, Newcastle University, Newcastle upon Tyne, UK

[3]Drug Discovery Unit, Wellcome Centre for Anti-Infectives Research, School of Life Sciences, University of Dundee, Dundee, UK

[4]Debiopharm, Lausanne, Switzerland

[5]Department of Forensic Genetics and Forensic Toxicology, National Board of Forensic Medicine, Linköping, Sweden

[6]Division of Clinical Chemistry and Pharmacology, Department of Biomedical and Clinical Sciences, Faculty of Medicine and Health Sciences, Linköping University, Linköping, Sweden

[7]Department of Natural Sciences, Manchester Metropolitan University, Manchester, UK

[8]Chiron AS, Trondheim, Norway

Correspondence
Andrew M. Brandon and Lorna A. Nisbet, Newcastle University Centre for Cancer, Newcastle University, Newcastle upon Tyne, UK.
Email: andrew.brandon@newcastle.ac.uk; lnisbet001@dundee.ac.uk

Present address
Andrew M. Brandon, Newcastle University Centre for Cancer, Newcastle University, Newcastle upon Tyne, UK.

Abstract

The emergence of new synthetic cannabinoid receptor agonists (SCRAs) onto the illicit drugs market continues to cause harm, and the overall availability of physico-chemical and pharmacokinetic data for new psychoactive substances is lacking. The lipophilicity of 23 SCRAs and the plasma protein binding (PPB) of 11 SCRAs was determined. Lipophilicity was determined using a validated chromatographic hydro-phobicity index (CHI) log D method; tested SCRAs showed moderate to high lipophilicity, with experimental log D$_{7.4}$ ranging from 2.48 (AB-FUBINACA) to 4.95 (4F-ABUTINACA). These results were also compared to in silico predictions generated using seven commercially available software packages and online tools (Canvas; ChemDraw; Gastroplus; MoKa; PreADMET; SwissADME; and XlogP). Licenced, dedicated software packages provided more accurate lipophilicity predictions than those which were free or had prediction as a secondary function; however, the latter still provided competitive estimates in most cases. PPB of tested SCRAs, as determined by equilibrium dialysis, was in the upper range of the lipophilicity scale, ranging from 90.8% (ADB-BUTINACA) to 99.9% (BZO-HEXOXIZID). The high PPB of these drugs may contribute to reduced rate of clearance and extended durations of pharmacological effects compared to lesser-bound SCRAs. The presented data improve understanding of the behaviour of these drugs in the body. Ultimately, similar data and predictions may be used in the prediction of the structure and properties of drugs yet to emerge on the illicit market.

KEYWORDS
lipophilicity, new psychoactive substances, pharmacokinetics, plasma protein binding, synthetic cannabinoid receptor agonists

1 | INTRODUCTION

Synthetic cannabinoid receptor agonists (SCRAs) are a large group of structurally diverse new psychoactive substances (NPS) that bind to and activate human cannabinoid receptors (CB_1 and CB_2).[1–4] Over 200 SCRAs encompassing a range of structural sub-classes have been detected in Europe since 2008,[5] SCRA consumption is observed worldwide,[2] and their detection and trend monitoring has been extensively reported.[5–13] While the use of SCRAs by the general population is low,[14,15] in many jurisdictions, including the United Kingdom, SCRA use in prisons, rough-sleeping populations and among those with a history of substance misuse remains common, with reasons for use varying between user groups.[6,14,16–20] In a prison context, SCRAs have been described as the NPS group of greatest concern.[6] The unpredictable effects of SCRAs, related to both the specific SCRA involved and the unpredictable concentration consumed, can result in significant physical, mental health and societal harm.[6,14,16,18] Adverse effects of SCRAs include agitation, aggression, seizures, loss of motor control and death.[21–24] Despite the documented harms of SCRAs, information on their physicochemical and pharmacokinetic properties is relatively limited. This poses challenges within the field of forensic toxicology that relies on understanding the efficacy and behaviour of analytes within the body to accurately interpret any concentrations identified.

Recent studies on the emergence and prevalence of SCRAs have demonstrated the transnational nature of SCRA emergence on illicit markets and the influence of national and international drug legislation.[2,19] Potent valinate and *tert*-leucinate indole and indazole-3-carboxamide SCRAs have dominated the illicit SCRA market in recent years, with many being brought under legislative control on a compound-by-compound basis.[25] Chinese legislation enacted in July 2021[26,27] sought to bring all valinate and *tert*-leucinate indole and indazole-3-carboxamide SCRAs under analogue-based legislative control for the first time. Despite this, some analogues, particularly ADB-BUTINACA (**2**) (ADB-BINACA; *N*-(1-amino-3,3-dimethyl-1-oxo-butan-2-yl)-1-butyl-1*H*-indazole-3-carboxamide) and MDMB-4en-PINACA (**5**) (methyl 3,3-dimethyl-2-[1-(pent-4-en-1-yl)-1*H*-indazole-3-carboxamido] butanoate), remain among the most prevalent SCRAs on the market[2,25] (SCRA compounds are numbered in bold throughout this text in the order provided in Figure 1). Following these legislative changes in China, the market responded by introducing a range of new SCRA structural sub-classes to market, which circumvent the legislation including the oxindole hydrazide-type ('OXIZID') SCRAs.[27–29] Additionally, producers have returned to analogues of previously introduced structural classes that had originally made little impact on the market, such as the pyrazole-5-carboxamides.[30]

Significant progress has been made in recent years to develop pharmacological structure–activity relationships (SARs) to determine the potency and efficacy of prevalent and emerging SCRAs, increasing understanding of their relative potential for harm.[23,25,31–41] Additionally, the application of in vitro metabolism techniques and the availability of confirmatory in vivo data from authentic case samples have allowed SCRA structure–metabolism relationships (SMRs) to be developed and in vivo metabolite structures to be predicted, identified and evaluated. This approach has efficiently identified the biomarkers of SCRA consumption and may in future lead to the in silico prediction of principal and/or unique metabolites to be identified as, or even before, new SCRAs emerge.[25,31–40] Despite the importance of fundamental physicochemical properties of SCRAs and their corresponding pharmacokinetic properties to their behaviour in the body after consumption, only a limited number of studies have offered comprehensive data on these factors.[9,42–46]

In general terms, the lipophilicity of a drug is an important predictor of the absorption, distribution, metabolism, elimination and toxicity (ADMET) characteristics of a drug and can be described by the partition coefficient (log P).[47,48] The higher the log P value, the more lipophilic the drug.[48] Lipophilicity influences the binding of SCRAs to plasma proteins, affecting their partitioning in the body, their volume of distribution, rate of metabolism and the duration of their psychoactive effects.[47] The distribution of a drug between compartments at physiological pH (pH 7.4) is described by the distribution coefficient (log $D_{7.4}$). When a drug is non-ionisable or is neutral at physiological pH, log P is equivalent to log $D_{7.4}$.[49]

The transport of SCRAs around the body via the bloodstream, and their deposition into longer-term storage sites such as adipose tissue, is highly dependent on their lipophilicity and the binding of SCRAs to blood plasma proteins, which is itself influenced by their lipophilicity.[47] Highly protein-bound drugs are not available to be metabolised or to exert their physiological effects, which in turn affects their duration of action and severity of the psychoactive effects experienced by the user.[50,51] Lipophilicity will also affect the likelihood of detecting a parent SCRA in urine and will affect the analytical detection windows of parent SCRAs and their metabolites in urine, blood and other toxicological samples.[50]

Given that there are many more theoretical molecular structures than it is possible to experimentally determine, the prediction of lipophilicity (and other physicochemical parameters such as pK_a) using in silico models has been an important aspect of pharmaceutical drug design for decades.[47] Common approaches have been based on the summation of lipophilicity contributions from individual molecular substructures/motifs,[47] but more recently, machine learning-based approaches have become increasingly common,[52,53] and a range of in-house, commercial and open access tools are now available to researchers.

This study presents a systematic approach designed to increase understanding of the fundamental physicochemical properties of SCRAs. These factors underpin the pharmacokinetic properties of SCRAs, and greater understanding supports the interpretation of analytical data in toxicology casework. A chromatographic hydrophobicity index (CHI) method was developed and validated to reliably determine the lipophilicity of a range of established and emerging SCRAs, improving the robustness of the presented data and building on previously published data.[42] Plasma protein binding (PPB) was determined experimentally using an established equilibrium dialysis methodology and combined with previously published data[42] to build a more extensive data set than previously available. Seven
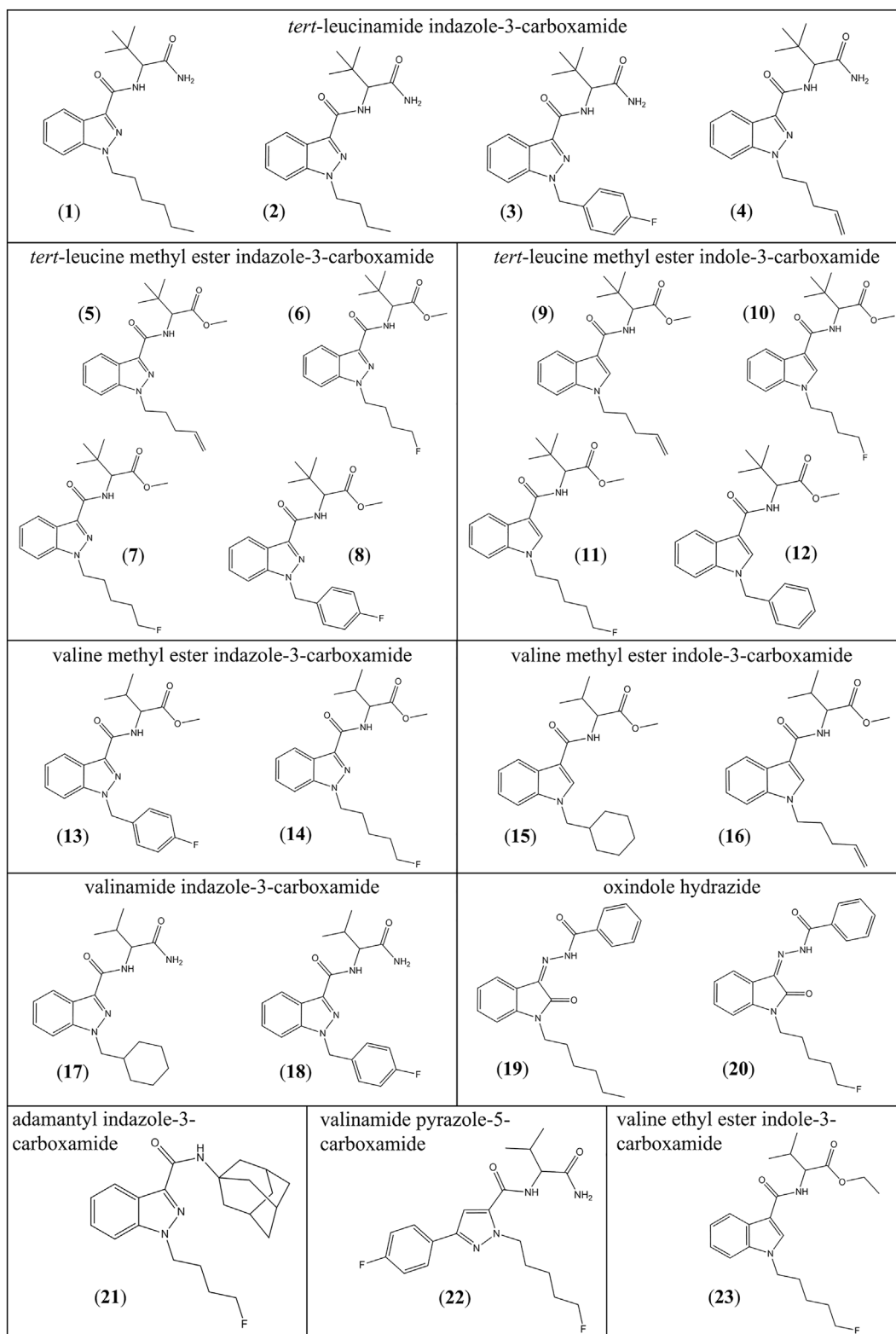
FIGURE 1 Structures and sub-classes of synthetic cannabinoid receptor agonists (SCRAs) involved in this study. (**1**) ADB-HEXINACA, (**2**) ADB-BUTINACA, (**3**) ADB-FUBINACA, (**4**) ADB-4en-PINACA, (**5**) MDMB-4en-PINACA, (**6**) 4F-MDMB-BUTINACA, (**7**) 5F-MDMB-PINACA, (**8**) MDMB-FUBINACA, (**9**) MDMB-4en-PICA, (**10**) 4F-MDMB-BUTICA, (**11**) 5F-MDMB-PICA, (**12**) MDMB-BENZICA, (**13**) MMB-FUBINACA, (**14**) 5F-MMB-PINACA, (**15**) MMB-CHMICA, (**16**) MMB-4en-PICA, (**17**) AB-CHMINACA, (**18**) AB-FUBINACA, (**19**) BZO-HEXOXIZID, (**20**) 5F-BZO-POXIZID, (**21**) 4F-ABUTINACA, (**22**) 5F-3,5-AB-PFUPPYCA, (**23**) 5F-EMB-PICA.

commercially available software packages and online tools designed to estimate lipophilicity in silico have been assessed in order to determine their reliability and suitability for the study of SCRAs. The ability of such experimental and in silico approaches to reliably predict the lipophilicity of SCRAs yet to emerge has been considered. The structures and sub-classes of the SCRAs included in this study are provided in Figure 1.

2 | MATERIALS AND METHODS

2.1 | Materials

2.1.1 | Reagents and controls

Ultra-high purity water (18 MΩ cm^{-1}) was obtained using a Milli-Q water purification system (Merck, Livingston, UK). Acetonitrile (LC-MS grade), methanol (LC-MS grade), ethanol (≥99.8% purity), dimethyl sulfoxide (DMSO) (≥99.9% purity), ammonium acetate (≥99% purity), formic acid (≥98% purity), donepezil hydrochloride (internal standard; ≥98% purity), phosphate-buffered saline tablets, bicinchoninic acid (BCA) protein assay kits, diazepam (positive control; ≥98% purity) and nicardipine hydrochloride (positive control; ≥98% purity) were purchased from Sigma-Aldrich (Gillingham, UK). Human plasma (pooled; Na EDTA anticoagulant, lot number IR07-081) [Innovative Research (Novi, MI, USA)] was purchased from Patricell (Nottingham, UK).

2.1.2 | Log D$_{7.4}$ calibration standards

Theophylline [certified reference material (CRM) grade], benzimidazole (≥98% purity), colchicine (CRM grade), phenyltheophylline (≥98% purity), acetophenone (≥99% purity), indole (≥99% purity), propiophenone (≥99% purity), butyrophenone (≥99% purity) and valerophenone (≥99% purity) were purchased from Sigma-Aldrich. Octanophenone (≥99% purity) and uracil (≥99% purity) were purchased from Thermo Fisher Scientific (Loughborough, UK).

2.1.3 | Test compounds

For all SCRAs possessing a chiral centre, reference materials used in the study comprised the (S)-enantiomer where applicable as seized samples tested have been shown to comprise almost exclusively the more potent (S)-enantiomer.[1] Unless otherwise stated, all purity data presented are chromatographic purity, rather than net purity. The enantiospecific synthesis of ADB-HEXINACA (1) (ADB-HINACA; N-(1-amino-3,3-dimethyl-1-oxobutan-2-yl)-1-hexyl-1H-indazole-3-carboxamide) (>99.5% purity), ADB-BUTINACA (2) (>98% purity), ADB-4en-PINACA (4) (ADB-PENINACA; N-(1-amino-3,3-dimethyl-1-oxobutan-2-yl)-1-(pent-4-en-1-yl)-1H-indazole-3-carboxamide) (>98% purity), MDMB-4en-PINACA (5) (>98.6% purity), 4F-MDMB-BUTINACA (6) (4F-ADB, 4F-MDMB-BINACA; methyl 2-[1-

(4-fluorobutyl)-1H-indazole-3-carboxamido]-3,3-dimethylbutanoate) (>99.7% purity), 5F-MDMB-PINACA (7) (5F-ADB; methyl 2-[1-(5-fluoropentyl)-1H-indazole-3-carboxamido]-3,3-dimethylbutanoate) (>99.6% purity), MDMB-FUBINACA (8) (methyl 2-[1-(4-fluorobenzyl)-1H-indazole-3-carboxamido]-3,3-dimethylbutanoate) (>99.9% purity), MDMB-4en-PICA (9) (methyl 3,3-dimethyl-2-[1-(pent-4-en-1-yl)-1H-indole-3-carboxamido]butanoate) (>99.7% purity), 5F-MDMB-PICA (11) (methyl 2-[1-(5-fluoropentyl)-1H-indole-3-carboxamido]-3,3-dimethylbutanoate) (>99% purity), MMB-FUBINACA (13) (AMB-FUBINACA; methyl [1-(4-fluorobenzyl)-1H-indazole-3-carbonyl]valinate) (>98% purity), 5F-MMB-PINACA (14) (5F-AMB, 5F-AMB-PINACA; methyl [1-(5-fluoropentyl)-1H-indazole-3-carbonyl]valinate) (>99.9% purity), MMB-CHMICA (15) (AMB-CHMICA; methyl [1-(cyclohexylmethyl)-1H-indole-3-carbonyl]valinate) (>99.6% purity), MMB-4en-PICA (16) (AMB-4en-PICA, MMB-022; methyl 3-methyl-2-[1-(pent-4-en-1-yl)-1H-indole-3-carboxamido]butanoate) (>99.7% purity), AB-CHMINACA (17) (N-[1-amino-3-methyl-1-oxobutan-2-yl]-1-(cyclohexylmethyl)-1H-indazole-3-carboxamide) (>99% purity), and AB-FUBINACA (18) (N-(1-amino-3-methyl-1-oxobutan-2-yl)-1-(4-fluorobenzyl)-1H-indazole-3-carboxamide) (>99% purity) has been described previously.[1,25,54,55] ADB-FUBINACA (3) (N-(1-amino-3,3-dimethyl-l-1-oxobutan-2-yl)-1-(4-fluorobenzyl)-1H-indazole-3-carboxamide) (93.7% net purity), BZO-HEXOXIZID (19) (MDA-19; (Z)-N'-(1-hexyl-2-oxoindolin-3-ylidene)benzohydrazide) (97.4% net purity), 4F-ABUTINACA (21) (N-(1-adamantyl)-1-(4-fluorobutyl)-1H-indazole-3-carboxamide) (99.9% net purity) and 5F-3,5-AB-PFUPPYCA (22) (AB-FUPPYCA; N-(1-amino-3-methyl-1-oxobutan-2-yl)-1-(5-fluoropentyl)-3-(4-fluorophenyl)-1H-pyrazole-5-carboxamide) (98.2% net purity) reference materials were purchased from Chiron AS (Trondheim, Norway). 5F-EMB-PICA (23) (ethyl 2-[[1-(5-fluoropentyl)indole-3-carbonyl]amino]-3-methylbutanoate) was purchased from Cayman Chemical Company (Michigan, USA) (>98% purity).

4F-MDMB-BUTICA (10) (4F-MDMB-BICA; methyl 2-[1-(4-fluorobutyl)-1H-indole-3-carboxamido]-3,3-dimethylbutanoate), MDMB-BENZICA (12) (methyl 2-[1-(benzyl)-1H-indole-3-carboxamido]-3,3-dimethylbutanoate) and 5F-BZO-POXIZID (20) (5F-MDA-19; (Z)-N'-(1-(5-fluoropentyl)-2-oxoindolin-3-ylidene)benzohydrazide) were produced in-house. Information relating to the synthesis and characterisation of these materials can be found in Section S1 of the Supporting Information.

Reference standard stock solutions were prepared in methanol or DMSO (solubility dependent) and stored at −20°C until use, unless used immediately.

2.2 | Methods

2.2.1 | Determination of CHI log D$_{7.4}$

The log D (pH 7.4) value for each SCRA involved in this study was determined using CHI measurements. A 100 μg mL^{-1} calibration mix for the CHI measurements, comprising 10 compounds with known log D$_{7.4}$ values (theophylline, benzimidazole, colchicine,

phenyltheophylline, acetophenone, indole, propiophenone, butyrophenone, valerophenone and octanophenone) plus uracil (an unretained compound) was prepared. SCRA and diazepam test compounds and controls were prepared individually at 1 mM in water: ACN (1:1 v/v). Preparation of the calibration mix and test solutions is described in greater detail in Section S2 of the Supporting Information.

The calibration mix and test compounds (n = 3) were analysed using high-performance liquid chromatography with photodiode array detection (HPLC-PDA) using an Agilent 1220 Infinity LC coupled to an Agilent 1220 photodiode array detector (Agilent Technologies, Stockport, UK). Data analysis was performed using OpenLAB CDS ChemStation Edition software (Agilent Technologies; version 1.159.23). All samples (5 μL) were injected onto a Zorbax SB-C$_{18}$ column (4.6 mm × 150 mm, 3.5 μm) (Agilent Technologies) at a flow rate of 1.2 mL min^{-1} at room temperature (25–29°C). The sample chamber was kept at room temperature (25–29°C). Gradient elution was performed, with a mobile phase (MP) consisting of ammonium acetate in water (10 mM, pH 7.4) (MP A) and acetonitrile (MP B). The following gradient was used: 0–12.0 min from 5% MP B to 95% MP B, 12.0–14.0 min hold 95% MP B, 14.0–14.5 min to 5% MP B, 14.5–16.0 min hold 5% MP B. Detection was achieved by scanning over a range of 190–400 nm wavelength, with 254 nm used for identification and peak area normalisation.

The calibration mix was analysed at the start and end of each test run, and the average retention times of the calibration compounds were used to calculate retention factors (k) according to Equation (1), which was then plotted against literature CHI values (CHI$_0$) for each compound.[56,57] Linear regression was used to obtain a line of best fit, from which the CHI was determined. CHI log D of calibration and test compounds were subsequently calculated according to Equation (2).

Calculation of retention factor (k):

$$k = \frac{(t_r - t_0)}{t_0} \quad (1)$$

where t_r is the retention time of the analyte and t_0 is the retention time of an unretained compound (uracil).

Calculation of CHI log D[58,59]:

$$CHI\,logD = (CHI \times 0.0525) - 1.467 \quad (2)$$

CHI log D method validation
Method validation of the CHI log D assay was carried out using the benzodiazepine drug diazepam and the SCRA MDMB-4en-PINACA (**5**) (1 mM in water: ACN (1:1 v/v)). The goodness of fit of a linear model to describe the relationship between retention factor and calculated CHI value was assessed using the coefficient of determination (R^2) values. Within-run (intra-day) precision was determined by triplicate analysis of the two test compounds analysed on the same day and is reported as the coefficient of variation (% CV). Evaluation of between-run (inter-day) precision was achieved by analysing the same test compounds on six non-consecutive days. The mean of the

calculated log D$_{7.4}$ values were thereafter defined as the true values, which were compared to the available literature data for diazepam and MDMB-4en-PINACA (**5**). The impact of analyte stability upon calculated log D$_{7.4}$ values was assessed. Autosampler stability was determined by re-injecting the test compounds at time 0, 24, 48 and 72 h. Samples were stored at room temperature (25–29°C) and injected in triplicate. Short-term freezer stability was assessed by storing the calibration mix and validation test compounds at −20°C for a 28-day period. The impact of three freeze–thaw cycles was also assessed. Accuracy was determined by calculation of % bias. Neat material and stock solution availability and concentration limitations determined the matrix composition of SCRA test solutions, with some containing up to 35% (v/v) methanol. To address this, the influence of 35% (v/v) methanol solvent in the calibration mix was compared to the usual 11% (v/v) DMSO to identify any differences in calibration standard retention times and thus calculated log D$_{7.4}$ values. This is detailed in Section S2 of the Supporting Information.

2.2.2 | In silico log P prediction

Log P for the SCRAs included in this study and for a range of proposed SCRAs was estimated using a range of software packages: Canvas (Schrödinger, LLC, New York, NY, USA; version 3.6), ChemDraw Professional (PerkinElmer, Waltham, MA, USA; version 20.1.1), Gastroplus (ADMET Predictor module) (Simulations Plus, Lancaster, CA, USA; version 9.8), MoKa (Molecular Discovery, Borehamwood, UK; version 3.0), PreADMET (Yonsei University, Seoul, Republic of Korea; online and open access), SwissADME (Swiss Institute of Bioinformatics, Lausanne, Switzerland; online and open access) and XlogP (Peking University, Beijing, China[60]; online and open access). The generated log P predictions were compared to experimental log D$_{7.4}$ data to identify the most accurate predictors. Statistical analysis was achieved using SPSS Statistics (IBM, Armonk, NY, USA; version 27) to generate root-mean-square error (RMSE) and Pearson correlations for comparison of predictive software to experimental data.

2.2.3 | In vitro PPB

PPB studies were performed using an established and previously validated equilibrium dialysis method using a 96-well dialysis block (HTDialysis, Ledyard, CT, USA).[42,61] Pooled human plasma (Innovative Research, Novi, MI, USA) was centrifuged (3750 rpm, 10 min, 22°C) to remove fibrin and used without further dilution. Plasma was spiked with either a test compound or with a positive control (nicardipine) (10 μg mL^{-1}; n ≥ 4) from stock solutions of either 10 mM in DMSO or 1 mg mL^{-1} in methanol, depending on reference material availability and solubility, and allowed to equilibrate (20 min, 22°C). Final solvent (DMSO or MeOH) concentrations never exceeded 1% (v/v). Spiked plasma (150 μL) was dialysed against isotonic phosphate buffer (pH 7.4) (150 μL) (100 rpm, 5 h, 37°C) using a Stuart SI60 benchtop incubator with shaking on a Stuart SSM1 mini orbital shaker (Cole-

Parmer, St. Neots, UK). Following incubation, dialysed plasma (50 μL) was added to drug-free buffer (50 μL), and dialysed buffer (50 μL) was added to drug-free plasma (50 μL). ACN (200 μL) containing donepezil as internal standard (IS, 50 ng mL^{-1}) was added to each sample, and samples were centrifuged (3750 rpm, 10 min, 22°C). The supernatant (150 μL) was added to deionised water (50 μL), and samples were subject to a further 10-fold dilution in water: ACN (1:1 v/v) to account for instrument sensitivity. Samples were analysed by ultra-performance liquid chromatography–tandem mass spectrometry (UPLC-MS/MS). BCA protein assay reagent was added to dialysed buffer from each well prior to general sampling to test for protein contamination to determine whether membranes had been compromised, according to manufacturer instructions. Nicardipine (positive control) PPB was compared to published data and previous in-house measurements.[42,62]

UPLC-MS/MS analysis was achieved using a Waters Acquity UPLC with a Waters Xevo TQS tandem mass spectrometer (Waters Ltd., Wilmslow, UK). Data analysis was performed using Waters MassLynx software (Waters Ltd.; version 4.1). Samples (0.2 μL; 5 μL for ADB-HEXINACA) were injected onto an Acquity BEH C$_{18}$ UPLC column (2.1 mm × 50 mm, 1.7 μm) (Waters Ltd.) at a flow rate of 0.6 mL min^{-1} at 45°C. The sample chamber was kept at 4°C. Gradient elution was performed, with MP A consisting of deionised water with formic acid (0.01% v/v) and MP B consisting of methanol with formic acid (0.01% v/v). The following gradient was used: 0–0.3 min 5% MP B, 0.3–1.3 min to 95% MP B, 1.3–1.79 min hold 95% MP B, 1.79–1.8 min to 5% MP B. For MS acquisition, positive electrospray ionisation (ESI) was used, with the MS operating in multiple reaction monitoring (MRM) mode. Source temperature was 150°C, desolvation gas was at 600°C with a flow rate of 1000 L h^{-1}, collision gas (nitrogen) flow rate was 0.15 mL min^{-1}, capillary voltage was 0.7 kV and cone gas flow rate was 150 L h^{-1}. Retention time, MRM transitions, cone voltage and collision energy for compounds included in PPB experiments are provided in Table 1.

Drug binding percentage and fraction unbound were calculated according to Equations (3) and (4), respectively.[63]

Calculation of percentage drug bound to plasma[63]:

$$\%bound = \frac{Pl - Bu}{Pl} \times 100 \qquad (3)$$

where Pl is the analyte/IS ratio in plasma side of well and Bu is the analyte/IS ratio in buffer side of well.

Calculation of fraction unbound[63]:

$$fu_P = \frac{(100 - \%bound)}{100} \qquad (4)$$

where fu_P is the fraction unbound in plasma.

3 | RESULTS AND DISCUSSION

3.1 | Lipophilicity

3.1.1 | CHI log D method validation

All validation data for the CHI log D assay are provided in Section S2 of the Supporting Information. Visual examination of the retention factor versus CHI$_0$ plots, residuals and R^2 values, which were ≥0.995 in all cases, indicate that the application of the linear model in this context was appropriate. True log D$_{7.4}$ values were determined for diazepam (2.90) and MDMB-4en-PINACA (5) (4.50). Previously reported experimental log D$_{7.4}$ values for diazepam (2.79–2.99)[63] and MDMB-4en-PINACA (5) (4.95)[42] are similar to those reported in this study. Intra-day and inter-day precision was deemed acceptable; % CV was ≤0.3% for both compounds. For the autosampler stability,

TABLE 1 Retention times, mass spectrometry multiple reaction monitoring transitions, cone voltages and collision energies for compounds included in the plasma protein binding study.

Compound	Retention time (min)	Transition (Da)	Cone voltage (V)	Collision energy (V)
ADB-HEXINACA (**1**)	1.63	358.83 - > 228.83	71	33
ADB-BUTINACA (**2**)	1.53	331.00 - > 201.08	38	26
ADB-FUBINACA (**3**)	1.51	383.08 - > 338.40	38	12
ADB-4en-PINACA (**4**)	1.54	342.96 - > 212.85	16	26
4F-MDMB-BUTICA (**10**)	1.53	363.03 - > 218.07	16	19
MDMB-BENZICA (**12**)	1.58	379.04 - > 90.82	16	40
BZO-HEXOXIZID (**19**)	1.72	350.08 - > 104.87	60	19
5F-BZO-POXIZID (**20**)	1.59	353.99 - > 104.86	16	19
4F-ABUTINACA (**21**)	1.69	370.11 - > 135.04	16	26
5F-3,5-AB-PFUPPYCA (**22**)	1.53	393.06 - > 188.99	16	33
5F-EMB-PICA (**23**)	1.55	377.07 - > 232.07	16	12
Nicardipine (+ve control)	1.28	480.06 - > 90.79	60	33
Donepezil (internal standard)	1.18	380.13 - > 90.80	60	33

Note: MRM transitions for other SCRA compounds included in PPB discussion have been previously published.[42]

short-term freezer stability and freeze–thaw cycle studies, all determined CHI log $D_{7.4}$ values were within ±0.3% of the true values.

Test compound matrix composition was influenced by the stock solution from which it was created; the presence of 35% (v/v) methanol or 11% (v/v) DMSO in the calibration mix produced no significant difference in calibration standard retention times and thus did not influence the calculated log $D_{7.4}$ values of calibration and test compounds (n = 2 for each calibration mix; % relative standard error ranged from 0.011% to 0.060%; unpaired t-test p-value ranged from 0.096 to 0.698). Calibration mix retention times and log $D_{7.4}$ values

for each matrix solvent composition are provided in Section S2 of the Supporting Information.

3.1.2 | Experimental CHI log $D_{7.4}$ and predicted log P

Log $D_{7.4}$ was determined using the validated HPLC-PDA method described above. Experimental log $D_{7.4}$ values for the tested SCRAs ranged from 2.48 (AB-FUBINACA (**18**), the least lipophilic) to 4.95

TABLE 2 Experimental log $D_{7.4}$ and predicted log P of synthetic cannabinoid receptor agonists.

Compound	Experimental CHI log $D_{7.4}$ (n = 3, ±SD)	Predicted log P							
		Gastroplus	MoKa	Canvas	ChemDraw log P	PreADMET	SwissADME	ChemDraw ClogP	XlogP
4F-ABUTINACA (**21**)	4.95 ± 0.00	**4.74**	4.70	4.17	3.57	4.50	4.36	4.30	4.68
BZO-HEXOXIZID (**19**)	4.88 ± 0.00	4.53	5.10	4.34	4.24	4.21	3.71	5.74	**5.01**
MDMB-4en-PINACA (**5**)	4.50 ± 0.01	3.61	4.00	3.69	3.82	4.02	3.41	**4.05**	3.87
MMB-CHMICA (**15**)	4.31 ± 0.01	4.48	**4.30**	4.53	3.84	4.76	3.84	5.49	5.51
MDMB-FUBINACA (**8**)	4.21 ± 0.01	**4.19**	4.10	4.08	4.33	4.41	3.83	4.52	4.24
5F-MDMB-PINACA (**7**)	4.09 ± 0.00	3.76	3.90	3.79	3.60	4.12	3.63	3.81	3.79
MDMB-4en-PICA (**9**)	3.98 ± 0.00	**3.98**	4.20	4.01	3.79	4.24	3.77	4.87	4.98
MMB-FUBINACA (**13**)	3.86 ± 0.00	3.75	3.80	**3.81**	3.79	4.14	3.50	4.12	4.09
4F-MDMB-BUTINACA (**6**)	3.82 ± 0.01	3.38	3.40	3.33	3.18	**3.67**	3.39	3.28	3.34
MDMB-BENZICA (**12**)	3.80 ± 0.00	4.28	4.20	4.20	4.13	4.43	**3.90**	4.75	5.25
ADB-HEXINACA (**1**)	3.78 ± 0.00	3.61	3.90	3.65	3.60	4.01	3.22	3.94	**3.77**
5F-MMB-PINACA (**14**)	3.73 ± 0.00	3.31	3.60	3.52	3.06	3.85	3.41	3.41	**3.64**
5F-MDMB-PICA (**11**)	3.67 ± 0.00	4.10	4.20	4.12	**3.57**	4.34	3.98	4.62	4.90
5F-BZO-POXIZID (**20**)	3.67 ± 0.00	3.82	4.20	**3.60**	3.33	3.47	3.42	4.49	4.18
5F-EMB-PICA (**23**)	3.63 ± 0.00	3.95	4.30	4.19	**3.36**	4.42	4.03	4.75	5.17
MMB-4en-PICA (**16**)	3.60 ± 0.00	3.50	3.90	3.74	3.25	3.97	**3.53**	4.47	4.83
4F-MDMB-BUTICA (**10**)	3.41 ± 0.01	3.69	3.70	**3.66**	3.15	3.89	3.67	4.10	4.45
AB-CHMINACA (**17**)	3.37 ± 0.00	3.12	3.10	**3.32**	2.96	3.69	2.91	3.55	3.55
ADB-4en-PINACA (**4**)	2.98 ± 0.00	2.61	**3.00**	2.80	2.91	3.17	2.68	2.93	3.02
ADB-BUTINACA (**2**)	2.92 ± 0.01	2.23	**2.90**	2.74	2.76	3.10	2.42	2.89	2.87
ADB-FUBINACA (**3**)	2.83 ± 0.00	**3.06**	3.20	3.20	3.41	3.56	3.10	3.40	3.39
5F-3,5-AB-PFUPPYCA (**22**)	2.77 ± 0.01	**2.76**	3.70	3.45	2.99	3.81	3.35	3.15	3.30
AB-FUBINACA (**18**)	2.48 ± 0.01	**2.66**	2.90	2.92	2.87	3.29	2.80	3.00	3.24
Root-mean-square error (in silico vs experimental)	n/a	0.35	0.38	0.40	0.49	0.50	0.50	0.66	0.76
Pearson correlation (in silico vs experimental)	n/a	0.854	0.828	0.771	0.746	0.730	0.709	0.714	0.607
Rank order	n/a	1	2	3	4	5	6	7	8
Accessibility	n/a	Paid[a]	Paid	Paid[b]	Paid	Free	Free	Paid	Free

Notes: **Bold** shows the most accurate prediction for each compound. Previously published data is shaded grey.[42]

[a]Feature also available through MedChem Designer software.

[b]Feature now part of LiveDesign software.

TABLE 3 Lipophilicity rank-order of synthetic cannabinoid receptor agonist structural moieties.

Lipophilicity rank (1 = most lipophilic)	Head group (code)	Core (code)	Tail group (code)
1	Adamantyl (A)	Indazole (INA)	Hexyl (HEX)
2	tert-Leucine methyl ester (MDMB)	Indole (I)	Cyclohexylmethyl (CHM)
3	Valine methyl ester (MMB)	—	4-Pentenyl (4en-P)
4	tert-Leucinamide (ADB)	—	Butyl (BUT)
5	Valinamide (AB)	—	p-Fluorobenzyl (FUB)
6	—	—	Benzyl (BENZ)
7	—	—	5-Fluoropentyl (5F-P)
8	—	—	4-Fluorobutyl (4F-BUT)

(4F-ABUTINACA (**21**), the most lipophilic), showing moderate to high lipophilicity[64] (Table 2). Data for individual replicates can be found in Section S3 of the Supporting Information.

The indole- and indazole-3-carboxamide SCRAs included in this study showed a wide range of log $D_{7.4}$ values. The high lipophilicity of 4F-ABUTINACA (**21**) (4.95) is due to the incorporation of the adamantyl head group, a commonly studied lipophilic structural moiety in drug design.[65] Experimental log $D_{7.4}$ for the tert-leucine methyl ester (MDMB-) SCRAs ranged from 3.4 to 4.5, valine methyl ester (MMB-) SCRAs ranged from 3.60 to 4.31, tert-leucinamide (ADB-) SCRAs ranged from 2.83 to 3.78, and valinamide (AB-) containing SCRAs ranged from 2.48 to 3.37. SCRAs with an indazole core tended to be more lipophilic than those with an indole core, for example, MDMB-4en-PINACA (**5**) (4.50) versus MDMB-4en-PICA (**9**) (3.98). SCRAs with a valinamide (AB-) or tert-leucinamide (ADB-) head group had log $D_{7.4}$ values of <3.40, with the exception of ADB-HEXINACA (**1**) (log $D_{7.4}$ = 3.78), most likely due to the influence of its more lipophilic hexyl tail group. These findings expand on previously published data[42] on a more limited set of SCRAs using a preliminary CHI log D method. Taking a systematic fragment approach and comparing the experimental log $D_{7.4}$ compounds where one structural motif changes at a time, a proposed ranking of the influence of SCRA subunits on lipophilicity is described in Table 3.

The experimental log $D_{7.4}$ values for BZO-HEXOXIZID (**19**) (4.88) and 5F-BZO-POXIZID (**20**) (3.67), reported here, to the best of the authors' knowledge, for the first time, support the observation that of the SCRA tail groups listed in Table 3, inclusion of a hexyl tail group in the SCRA structure increases the overall lipophilicity of a SCRA, if all other structural motifs remain constant. Due to their relatively high lipophilicity, it is suggested that these two SCRAs are less likely to be detected in urine, and if so, at low proportions relative to their more polar metabolites.[66,67] In addition, the log $D_{7.4}$ of a pyrazole-5-carboxamide (5F-3,5-AB-PFUPPYCA (**22**), 2.77) is also reported for the first time. This is the second lowest log $D_{7.4}$ value of all the SCRAs reported here; this lower lipophilicity is likely influenced by the inclusion of a pyrazole core instead of indole or indazole group, and the inclusion of a valinamide (AB) head group. It is therefore suggested that the 5F-3,5-AB-PFUPPYCA (**22**) parent drug may be detected in urine at relatively high proportions compared to more lipophilic SCRAs, as is observed for AB-FUBINACA (**18**),[68] although the

metabolic stability of 5F-3,5-AB-PFUPPYCA (**22**) and the identity of its metabolites have not yet been reported.

Due to their relatively high lipophilicity, it is likely that some of the SCRAs reported here will distribute into the adipose tissue, especially those with greater metabolic stability.[42] This means that accumulation of the parent drug in lipid-rich adipose tissue of chronic users with redistribution back into systemic circulation at a later time is possible, thus extending their (and their metabolites) detection windows.[9,43,69] With increasing lipophilicity, the chance of detecting SCRA parent compounds in the urine decreases, and it has been suggested that it may not be possible to detect parent SCRAs with log $D_{7.4}$ or log P values of around 4–5 or greater in this matrix.[66]

From a pharmacokinetic perspective, SCRA lipophilicity will influence a wide range of ADMET properties. More lipophilic SCRAs may more easily cross the airway epithelium via passive transport[70] and may also have increased oral absorption.[48] Log P values of between 2 and 5 can contribute to increased blood–brain barrier penetration through increased transmembrane diffusion and, for drugs with a molecular weight of <400 Da, reduced P-glycoprotein efflux.[48,71] SCRAs with lower lipophilicity will be more metabolically stable against cytochrome P450 (CYP) metabolism, glucuronidation and sulfation,[72] with inclusion of a fluorine also reducing CYP-mediated biotransformation,[48] as previously demonstrated.[42]

A small number of studies have used in silico methods to predict the log P of SCRAs. The available data predicts SCRAs to have moderate to very high lipophilicity, with estimated log P values ranging from 1.57 to 8.14.[42,66,69,73,74] SCRAs containing methylnaphthyl, naphthyl and quinolin-8-yl head groups have significantly higher predicted log P values than those SCRAs reported here [e.g. JWH-210 (log P = 8.14), MAM2201 (6.88), NM2201 (6.74) and PB-22 (6.53)].[66] Predicted log P values obtained in this study, using seven distinct software packages and online tools, range from 2.23 (ADB-BUTINACA (**2**), Gastroplus) to 5.74 (BZO-HEXOXIZID (**19**), ChemDraw ClogP), and the data were combined with data from a previous study for additional SCRAs[42] (Table 2).

While the most accurate predictions (comparison of experimentally derived values generated in this study to in silico predicted values) for each individual compound varied (given in bold in Table 2), Gastroplus software provided the most accurate predictions overall

FIGURE 2 Correlation between experimental log $D_{7.4}$ ($n = 3$) and log P prediction by the three best performing software packages (a) Gastroplus; (b) MoKa; (c) Canvas software packages.
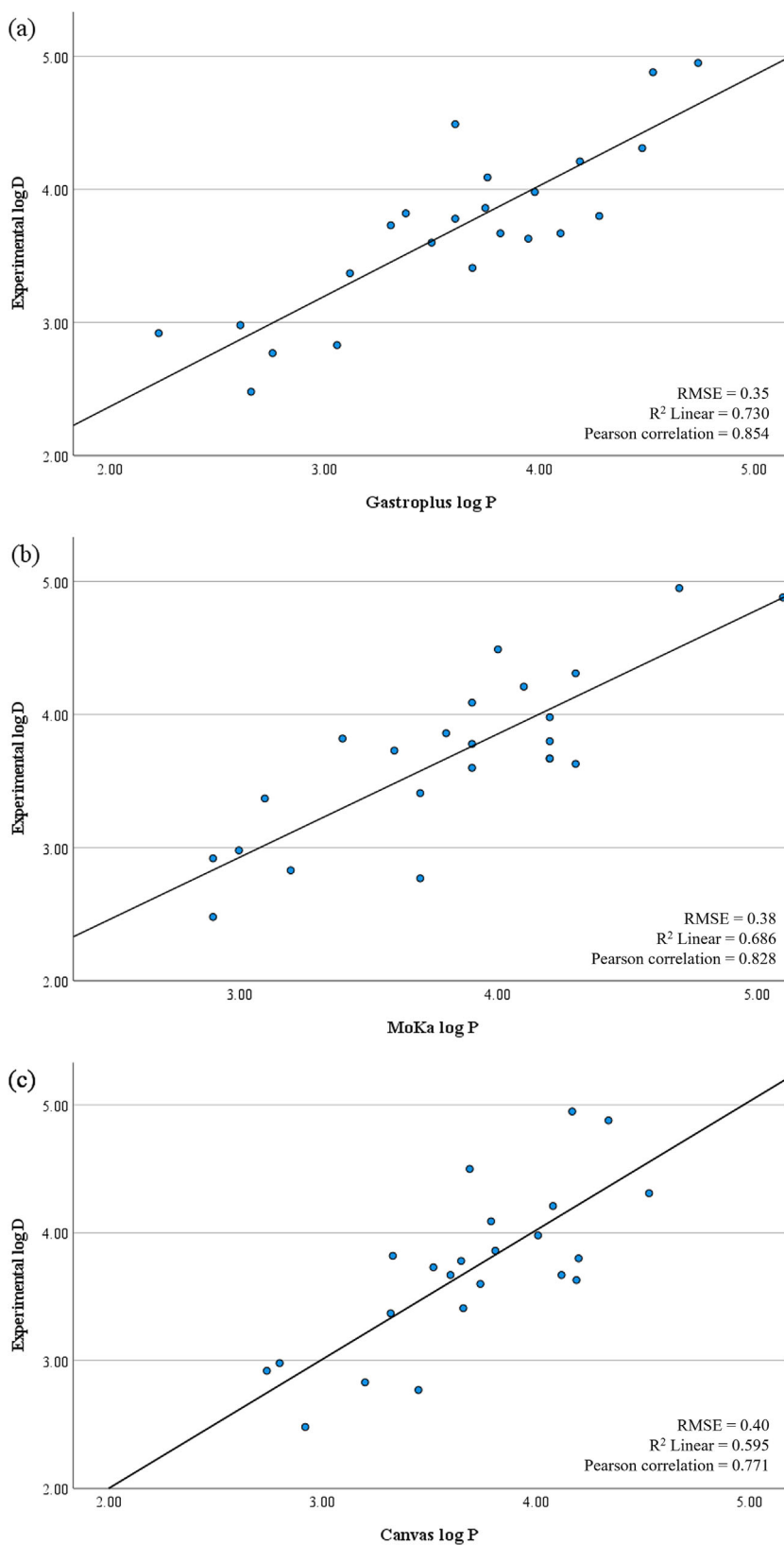
(RMSE = 0.35), closely followed by MoKa (RMSE = 0.38) and Canvas (RMSE = 0.40) [now integrated into LiveDesign (Schrödinger) software]. In order of prediction accuracy, other software packages and online tools used were ChemDraw (log P function) (RMSE = 0.49), PreADMET (online) (RMSE = 0.50), SwissADME (online) (RMSE = 0.50), ChemDraw (ClogP function) (RMSE = 0.66) and XlogP

TABLE 4 Experimental and literature plasma protein binding (PPB) of synthetic cannabinoid receptor agonists.

| Compound | Experimental | | | Literature |
	PPB (%)	Fraction unbound (fu_P)	n	PPB (%)
BZO-HEXOXIZID (19)	99.9 ± 0.01	0.001 ± 0.0001	4	—
ADB-HEXINACA (1)	99.7 ± 0.08	0.003 ± 0.0008	4	—
4F-ABUTINACA (21)	99.6 ± 0.19	0.004 ± 0.0019	4	—
MDMB-FUBINACA (8)	—	—	—	99.5 ± 0.08 [42]
MDMB-BENZICA (12)	99.1 ± 0.09	0.009 ± 0.0009	4	—
MDMB-4en-PINACA (5)	—	—	—	99.0 ± 0.01 [42]
JWH-018	—	—	—	99 [74]
JWH-210	—	—	—	99 [74]
AM-2201	—	—	—	99 [74]
RCS-4	—	—	—	99 [74]
WIN-55,212-2	—	—	—	99 [74]
5F-BZO-POXIZID (20)	98.9 ± 0.22	0.011 ± 0.0022	4	—
MMB-CHMICA (15)	—	—	—	98.8 ± 0.06 [42]
MMB-FUBINACA (13)	—	—	—	98.1 ± 0.08 [42]
JWH-200	—	—	—	98 [42]
AB-FUBINACA (18)	—	—	—	97.9 ± 0.44 [42]
5F-MDMB-PINACA (7)	—	—	—	97.8 ± 0.19 [42]
5F-EMB-PICA (23)	97.4 ± 0.24	0.026 ± 0.0024	4	—
AB-CHMINACA (17)	—	—	—	97.2 ± 2.19 [42]
MDMB-4en-PICA (9)	—	—	—	96.5 ± 0.32 [42]
4F-MDMB-BUTICA (10)	95.2 ± 0.49	0.048 ± 0.0049	4	—
ADB-FUBINACA (3)	95.1 ± 3.12	0.049 ± 0.0312	6	—
MMB-4en-PICA (16)	—	—	—	94.7 ± 0.37 [42]
5F-MMB-PINACA (14)	—	—	—	94.2 ± 0.08 [42]
4F-MDMB-BUTINACA (6)	—	—	—	93.9 ± 0.28 [42]
5F-MDMB-PICA (11)	—	—	—	93.8 ± 0.07 [42]
5F-3,5-AB-PFUPPYCA (22)	93.0 ± 1.13	0.070 ± 0.0113	4	—
ADB-4en-PINACA (4)	92.9 ± 1.65	0.071 ± 0.0165	6	—
ADB-BUTINACA (2)	90.8 ± 3.72	0.092 ± 0.0372	6	—
5F-AB-PINACA	—	—	—	87 [74]

(RMSE = 0.76). The correlation between experimental log $D_{7.4}$ and predicted log P for the three best-performing software packages, Gastroplus, MoKa and Canvas, is shown in Figure 2a–c, respectively.

Commercially available software packages dedicated to physico-chemical and pharmacokinetic parameter predictions (i.e. Gastroplus, MoKa and Canvas) produced predicted lipophilicity data that were most similar to experimental data generated in this study, however the open access resources (PreADMET, SwissADME and XlogP) provided competitive results and offer accessible and affordable alternatives. ChemDraw, which offers log P prediction as a secondary function, showed similar prediction accuracy to PreADMET and SwissADME for the SCRAs tested.

The rapidly evolving nature of the NPS market creates challenges for researchers, clinicians, toxicologists and drug monitoring agencies alike, with new drug compounds regularly emerging on the market. The ability to predict the physicochemical and pharmacokinetic properties of drugs in silico—a practice increasingly employed in modern drug discovery[52]—improves understanding of drug properties and can save significant amounts of time and money. Predictions would aid the interpretation of analytical toxicology data, where the lipophilicity of a compound will impact its window of detection and the likelihood of detecting the parent compound in different matrices, as well as the chosen sample extraction method prior to analysis. The presented approach allows the ranking of SCRAs in terms of lipophilicity, and greater value in the data set is derived from understanding of the properties of individual compounds relative to one another. Knowledge on the accuracy and error rates of different in silico tools increases confidence in their use by researchers. Experimentally derived data using fully validated analytical methods of known quality, such as that presented in this study, should be used as reference data for improving current software algorithms for specific emerging illicit drug classes such as the SCRAs.

3.2 | PPB

PPB is an important factor in drug pharmacokinetics, strongly influencing drug distribution between tissues and in vivo clearance.[51] Experimental data on the PPB of SCRAs is scarce. Previous work, using the same methodology employed in this study, showed indole and indazole-3-carboxamide SCRAs to be highly protein bound, with PPB ranging from 93.8% to 99.5%.[42] Leibnitz[75] reported the PPB of a range of older-generation SCRAs using an ultrafiltration method, where binding was also found to be high—98%–99%, likely influenced by their often high predicted lipophilicity.[66] The PPB of 5F-AB-PINACA was reported to be 87%,[75] slightly lower than the compounds included in this study and supporting observations from this and an earlier study[42] that valinamide (AB-) SCRAs are among the least lipophilic of all of the SCRAs. Experimental and literature PPB values for a wide range of SCRAs are provided in Table 4. The full experimental data set for the compounds reported in this study for the first time is provided in Section S4 of the Supporting Information.

In this study, the positive control, nicardipine, gave a PPB range of 98.3 ± 1.01% ($n = 9$), in line with literature data[62] (98%–99.5%) and previously observed in-house values[42] (97.7%–99.5%). The PPB of the tested SCRAs ranged from 90.8% (ADB-BUTINACA (**2**)) to 99.9% (BZO-HEXOXIZID (**19**)), showing a high degree of binding (Table 4). The lowest PPB value for the OXIZID-type SCRAs, reported here for the first time, was 98.9% (5F-BZO-POXIZID (**20**)), suggesting that this class of compound is particularly highly plasma protein bound. The degree of PPB correlated with experimental log $D_{7.4}$ (Pearson correlation = 0.637), with higher lipophilicity generally resulting in higher PPB values; however, other factors will contribute to individual differences in rank order (such as other physicochemical properties and affinity for different proteins).

Despite many SCRAs being susceptible to rapid metabolism by hepatic enzymes,[42] their high degree of PPB means that their half-life in the blood will be extended and only a small proportion of the dose may be available to exert a pharmacological response or become metabolised to more polar metabolites. Toxicological detection windows of SCRAs will therefore be longer than their metabolic stability alone would indicate.[42,51] However, while increasing lipophilicity can lead to increased PPB, more lipophilic drugs are generally less metabolically stable, and so lipophilicity alone is not a reliable indicator of whole-body clearance.[42,76] Despite the low proportion of freely circulating parent compound, as indicated by their high degree of PPB, many of these drugs exhibit high cannabinoid receptor binding and potency and exert a strong pharmacological response in users.[27,54,77]

4 | CONCLUSION

An HPLC-PDA method for determining CHI log D was developed, fully validated and applied to determine the lipophilicity of a wide range of SCRAs. The tested SCRAs showed moderate to high lipophilicity, which will influence a range of ADMET characteristics, including their distribution in the body. Assessment of the accuracy of log $D_{7.4}$ values predicted using several software packages and online tools demonstrated that, for the SCRAs included in the study, licenced software packages developed and designed specifically for prediction and modelling in drug development produced in silico data that was, overall, more comparable to experimental data than open access or non-specialised software. However, some less costly or free in silico options were still able to predict lipophilicity with reasonable accuracy and may be considered as more accessible alternatives. All SCRAs tested were highly bound to plasma proteins, a property that will increase their in vivo half-lives. With increasing interest in the use of in silico prediction of drug properties in areas such as drug discovery, toxicology research and analytical toxicology data interpretation, the availability of reference data sets and predictive in silico software packages of known performance against ground truth data is of great benefit.

CONFLICT OF INTEREST STATEMENT

CM is employed by Chiron AS, a producer of commercially available analytical reference materials. All Chiron AS reference standards used were purchased for inclusion in the study. CP is a shareholder in Simulations Plus, which produces and licences Gastroplus, one of the software packages utilised for prediction of lipophilicity in this study. The remaining authors do not report any conflicts of interest.

ORCID

Steven R. Baginski https://orcid.org/0000-0001-5615-1199
Henrik Green https://orcid.org/0000-0002-8015-5728
Oliver B. Sutcliffe https://orcid.org/0000-0003-3781-7754
Niamh Nic Daéid https://orcid.org/0000-0002-9338-0887
Lorna A. Nisbet https://orcid.org/0000-0002-8789-9113

REFERENCES

1. Antonides LH, Cannaert A, Norman C, et al. Shape matters: the application of activity-based in vitro bioassays and chiral profiling to the pharmacological evaluation of synthetic cannabinoid receptor agonists in drug-infused papers seized in prisons. *Drug Test Anal*. 2021; 13(3):628-643. doi:10.1002/dta.2965
2. Norman C, Halter S, Haschimi B, et al. A transnational perspective on the evolution of the synthetic cannabinoid receptor agonists market: comparing prison and general populations. *Drug Test Anal*. 2021; 13(4):841-852. doi:10.1002/dta.3002
3. Banister SD, Connor M. The chemistry and pharmacology of synthetic cannabinoid receptor agonists as new psychoactive substances: origins. Maurer HH, Brandt SD, eds. *Handb Exp Pharmacol*. 2018;252: 165-190. doi:10.1007/164_2018_143
4. Cannaert A, Sparkes E, Pike E, et al. Synthesis and in vitro cannabinoid receptor 1 activity of recently detected synthetic cannabinoids 4F-

MDMB-BICA, 5F-MPP-PICA, MMB-4en-PICA, CUMYL-CBMICA, ADB-BINACA, APP-BINACA, 4F-MDMB-BINACA, MDMB-4en-PINACA, A-CHMINACA, 5F-AB-P7AICA, 5F-MDMB-P7AICA, and 5F-AP7AICA. *ACS Chem Nerosci*. 2020;11(24):4434-4446. doi:10.1021/acschemneuro.0c00644

5. European Monitoring Centre for Drugs and Drug Addiction. European drug report 2022: trends and developments. European Union; 2022:60.

6. Norman C, Walker G, McKirdy B, et al. Detection and quantitation of synthetic cannabinoid receptor agonists in infused papers from prisons in a constantly evolving illicit market. *Drug Test Anal*. 2020; 12(4):538-544. doi:10.1002/dta.2767

7. Al-Matrouk A, Algallaf M, AlShemmeri A, BoJbarah H. Identification of synthetic cannabinoids that were seized, consumed, or associated with deaths in Kuwait in 2018 using GC-MS and LC-MS-MS analysis. *Forensic Sci Int*. 2019;303:109960. doi:10.1016/j.forsciint.2019.109960

8. Somerville RF, Hassan VR, Kolbe E, et al. The identification and quantification of synthetic cannabinoids seized in New Zealand in 2017. *Forensic Sci Int*. 2019;300:19-27. doi:10.1016/j.forsciint.2019.04.014

9. Schaefer N, Nordmeier F, Kröll AK, et al. Is adipose tissue suitable for detection of (synthetic) cannabinoids? A comparative study analyzing antemortem and postmortem specimens following pulmonary administration of JWH-210, RCS-4, as well as Δ9-tetrahydrocannabinol to pigs. *Arch Toxicol*. 2020;94(10):3421-3431. doi:10.1007/s00204-020-02843-x

10. Haschimi B, Mogler L, Halter S, et al. Detection of the recently emerged synthetic cannabinoid 4F-MDMB-BINACA in "legal high" products and human urine specimens. *Drug Test Anal*. 2019;11(9): 1377-1386. doi:10.1002/dta.2666

11. Castaneto MS, Wohlfarth A, Desrosiers NA, Hartman RL, Gorelick DA, Huestis MA. Synthetic cannabinoids pharmacokinetics and detection methods in biological matrices. *Drug Metab Rev*. 2015; 47(2):124-174. doi:10.3109/03602532.2015.1029635

12. Giorgetti A, Mogler L, Haschimi B, et al. Detection and phase I metabolism of the 7-azaindole-derived synthetic cannabinoid 5F-AB-P7AICA including a preliminary pharmacokinetic evaluation. *Drug Test Anal*. 2020;12(1):78-91. doi:10.1002/dta.2692

13. Mogler L, Franz F, Rentsch D, et al. Detection of the recently emerged synthetic cannabinoid 5F-MDMB-PICA in "legal high" products and human urine samples. *Drug Test Anal*. 2017;10(1):196-205. doi:10.1002/dta.2201

14. Gray P, Ralphs R, Williams L. The use of synthetic cannabinoid receptor agonists (SCRAs) within the homeless population: motivations, harms and the implications for developing an appropriate response. *Addict Res Theory*. 2021;29(1):1-10. doi:10.1080/16066359.2020.1730820

15. Jackson MA, Brown AL, Johnston J, et al. The use and effects of synthetic cannabinoid receptor agonists by New South Wales cannabis treatment clients. *J Cannabis Res*. 2021;3(1):33. doi:10.1186/s42238-021-00091-z

16. Ralphs R, Williams L, Askew R, Norton A. Adding spice to the porridge: the development of a synthetic cannabinoid market in an English prison. *Int J Drug Policy*. 2017;40:57-69. doi:10.1016/j.drugpo.2016.10.003

17. European Monitoring Centre for Drugs and Drug Addiction. New psychoactive substances in prison. European Union; 2018. https://www.emcdda.europa.eu/system/files/publications/8869/nps-in-prison.pdf

18. Ralphs R, Gray P, Sutcliffe OB. The impact of the 2016 psychoactive substances act on synthetic cannabinoid use within the homeless population: markets, content and user harms. *Int J Drug Policy*. 2021; 97:103305. doi:10.1016/j.drugpo.2021.103305

19. Rodrigues TB, Souza MP, Barbosa LM, et al. Synthetic cannabinoid receptor agonists profile in infused papers seized in Brazilian prisons. *Forensic Toxicol*. 2022;40(1):119-124. doi:10.1007/s11419-021-00586-7

20. Smith KE, Staton M. Synthetic cannabinoid use among a sample of individuals enrolled in community-based recovery programs: are synthetic cannabinoids actually preferred to other drugs? *Subst Abus*. 2019;40(2):160-169. doi:10.1080/08897077.2018.1528495

21. Trecki J, Gerona RR, Schwartz MD. Synthetic cannabinoid-related illnesses and deaths. *NEJM*. 2015;373(2):103-107. doi:10.1056/nejmp1505328

22. Adams AJ, Banister SD, Irizarry L, Trecki J, Schwartz M, Gerona R. "Zombie" outbreak caused by the synthetic cannabinoid AMB-FUBINACA in New York. *NEJM*. 2017;376(3):235-242. doi:10.1056/NEJMoa1610300

23. Sherpa D, Paudel BM, Subedi BH, Chow RD. Synthetic cannabinoids: the multi-organ failure and metabolic derangements associated with getting high. *J Community Hosp Intern Med Perspect*. 2015;5(4):27540. doi:10.3402/jchimp.v5.27540

24. Kolla NJ, Mishra A. The endocannabinoid system, aggression, and the violence of synthetic cannabinoid use, borderline personality disorder, antisocial personality disorder, and other psychiatric disorders. *Front Behav Neurosci*. 2018;12:41. doi:10.3389/fnbeh.2018.00041

25. Kronstrand R, Norman C, Vikingsson S, et al. The metabolism of the synthetic cannabinoids ADB-BUTINACA and ADB-4en-PINACA and their detection in forensic toxicology casework and infused papers seized in prisons. *Drug Test Anal*. 2022;14(4):634-652. doi:10.1002/dta.3203

26. The Associated Press. China issues total ban on synthetic cannabinoids. 2021. https://abcnews.go.com/Health/wireStory/china-issues-total-ban-synthetic-cannabinoids-77617434

27. Deventer MH, Van Uytfanghe K, Vinckier IMJ, Reniero F, Guillou C, Stove CP. Cannabinoid receptor activation potential of the next generation, generic ban evading OXIZID synthetic cannabinoid receptor agonists. *Drug Test Anal*. 2022;14(9):1565-1575. doi:10.1002/dta.3283

28. Liu CM, Hua ZD, Jia W, Li T. Identification of AD-18, 5F-MDA-19, and pentyl MDA-19 in seized materials after the class-wide ban of synthetic cannabinoids in China. *Drug Test Anal*. 2021;14(2):307-316. doi:10.1002/dta.3185

29. Schelkun RM, Krotulski AJ, Iula DM, Logan BK. New systematic naming for synthetic cannabinoid "MDA-19" and its related analogues: BZO-HEXOXIZID, 5F-BZO-POXIZID, and BZO-POXIZID. NPS Discovery; 2021. https://www.npsdiscovery.org/wp-content/uploads/2021/08/New-Systematic-Naming-for-MDA-19-and-Related-Analogues_NPS-Discovery_083121.pdf

30. Norman C, Reid R, Hill K, Cruickshanks F, Daeid NN. Newly emerging synthetic cannabinoids and novel modes of use of benzodiazepines in prisons: an update from the Scottish prisons non-judicial seizures drug monitoring project. *Toxicol Anal Clin*. 2022;34(3, Supplement): S150. doi:10.1016/j.toxac.2022.06.253

31. Diao X, Huestis MA. New synthetic cannabinoids metabolism and strategies to best identify optimal marker metabolites. *Front Chem*. 2019;7:109. doi:10.3389/fchem.2019.00109

32. Andersson M, Diao X, Wohlfarth A, Scheidweiler KB, Huestis MA. Metabolic profiling of new synthetic cannabinoids AMB and 5F-AMB by human hepatocyte and liver microsome incubations and high-resolution mass spectrometry. *RCM*. 2016;30(8):1067-1078. doi:10.1002/rcm.7538

33. Yeter O, Ozturk YE. Metabolic profiling of synthetic cannabinoid 5F-ADB by human liver microsome incubations and urine samples using high-resolution mass spectrometry. *Drug Test Anal*. 2018;11(6):847-858. doi:10.1002/dta.2566

34. Presley BC, Castaneto MS, Logan BK, Jansen-Varnum SA. Metabolic profiling of synthetic cannabinoid 5F-ADB and identification of metabolites in authentic human blood samples via human liver microsome incubation and ultra-high performance liquid

chromatography/high-resolution mass spectrometry. *RCM*. 2020; 34(22):e8908. doi:10.1002/rcm.8908

35. Presley BC, Logan BK, Jansen-Varnum SA. In vitro phase I metabolism of indazole carboxamide synthetic cannabinoid MDMB-CHMINACA via human liver microsome incubation and high-resolution mass spectrometry. *Drug Test Anal*. 2019;11(8):1264-1276. doi:10.1002/dta.2615

36. Presley BC, Castaneto MS, Logan BK, Jansen-Varnum SA. Assessment of synthetic cannabinoid FUB-AMB and its ester hydrolysis metabolite in human liver microsomes and human blood samples by UHPLC-MS/MS. *Biomed Chromatogr*. 2020;34(9):e4884. doi:10.1002/bmc.4884

37. Wohlfarth A, Castaneto MS, Zhu M, et al. Pentylindole/pentylindazole synthetic cannabinoids and their 5-fluoro analogs produce different primary metabolites: metabolite profiling for AB-PINACA and 5F-AB-PINACA. *AAPS j*. 2015;17(3):660-677. doi:10.1208/s12248-015-9721-0

38. Carlier J, Diao X, Wohlfarth A, Scheidweiler K, Huestis MA. In vitro metabolite profiling of ADB-FUBINACA, a new synthetic cannabinoid. *Curr Neuropharmacol*. 2017;15(5):682-691. doi:10.2174/1570159X15666161108123419

39. Watanabe S, Vikingsson S, Åstrand A, Gréen H, Kronstrand R. Biotransformation of the new synthetic cannabinoid with an alkene, MDMB-4en-PINACA, by human hepatocytes, human liver microsomes, human urine and blood. *AAPS j*. 2020;22(1):1-9, 13. doi:10.1208/s12248-019-0381-3

40. Watanabe S, Wu X, Dahlen J, et al. Metabolism of MMB022 and identification of dihydrodiol formation in vitro using synthesized standards. *Drug Test Anal*. 2020;12(10):1432-1441. doi:10.1002/dta.2888

41. Giorgetti A, Busardò FP, Tittarelli R, Auwärter V, Giorgetti R. Postmortem toxicology: a systematic review of death cases involving synthetic cannabinoid receptor agonists. *Front Psych*. 2020;11:464. doi:10.3389/fpsyt.2020.00464

42. Brandon AM, Antonides LH, Riley J, et al. A systematic study of the in vitro pharmacokinetics and estimated human in vivo clearance of indole and indazole-3-carboxamide synthetic cannabinoid receptor agonists detected on the illicit drug market. *Molecules*. 2021;26(5): 1396. doi:10.3390/molecules26051396

43. Franz F, Haschimi B, King LA, Auwärter V. Extraordinary long detection window of a synthetic cannabinoid metabolite in human urine - potential impact on therapeutic decisions. *Drug Test Anal*. 2020;12(3): 391-396. doi:10.1002/dta.2770

44. Gaunitz F, Lehmann S, Thomas A, Thevis A, Rothschild MA, Mercer-Chalmers-Bender K. Post-mortem distribution of the synthetic cannabinoid MDMB-CHMICA and its metabolites in a case of combined drug intoxication. *Int J Leg Med*. 2018;132(6):1645-1657. doi:10.1007/s00414-018-1911-8

45. Krotulski AJ, Garibay N, Walther D, et al. Pharmacokinetics and pharmacodynamics of the synthetic cannabinoid, 5F-MDMB-PICA, in male rats. *Neuropharmacology*. 2021;199:108800. doi:10.1016/j.neuropharm.2021.108800

46. Schaefer N, Wojtyniak JG, Kettner M, et al. Pharmacokinetics of (synthetic) cannabinoids in pigs and their relevance for clinical and forensic toxicology. *Toxicol Lett*. 2016;253:7-16. doi:10.1016/j.toxlet.2016.04.021

47. Soares JX, Santos Á, Fernandes C, Pinto MMM. Liquid chromatography on the different methods for the determination of lipophilicity: an essential analytical tool in medicinal chemistry. *Chem*. 2022;10(8): 340. doi:10.3390/chemosensors10080340

48. Schnider P. Overview of strategies for solving ADMET challenges. In: *The Medicinal Chemist's Guide to Solving ADMET Challenges*. Royal Society of Chemistry; 2021. Accessed 25 January 2023. doi:10.1039/9781788016414-00001https://books.rsc.org/books/edited-volume/779/chapter/426943/Overview-of-Strategies-for-Solving-ADMET

49. Hill AP, Young RJ. Getting physical in drug discovery: a contemporary perspective on solubility and hydrophobicity. *Drug Discov Today*. 2010;15(15):648-655. doi:10.1016/j.drudis.2010.05.016

50. Zhang F, Xue J, Shao J, Jia L. Compilation of 222 drugs' plasma protein binding data and guidance for study designs. *Drug Discov Today*. 2012;17(9–10):475-485. doi:10.1016/j.drudis.2011.12.018

51. Bohnert T, Gan LS. Plasma protein binding: from discovery to development. *J Pharm Sci*. 2013;102(9):2953-2994. doi:10.1002/jps.23614

52. Shaker B, Ahmad S, Lee J, Jung C, Na D. In silico methods and tools for drug discovery. *Comput Biol Med*. 2021;137:104851. doi:10.1016/j.compbiomed.2021.104851

53. Mannhold R, Poda GI, Ostermann C, Tetko IV. Calculation of molecular lipophilicity: state-of-the-art and comparison of log P methods on more than 96,000 compounds. *J Pharm Sci*. 2009;98(3):861-893. doi:10.1002/jps.21494

54. Antonides LH, Cannaert A, Norman C, et al. Enantiospecific synthesis, chiral separation, and biological activity of four indazole-3-carboxamide-type synthetic cannabinoid receptor agonists and their detection in seized drug samples. *Front Chem*. 2019;7:321. doi:10.3389/fchem.2019.00321

55. Gilbert N, Costello A, Ellison JR, et al. Synthesis, characterisation, detection and quantification of a novel hexyl-substituted synthetic cannabinoid receptor agonist: (S)-N-(1-amino-3,3-dimethyl-1-oxobutan-2-yl)-1-hexyl-1H-indazole-3-carboxamide (ADB-HINACA). *Forensic Chem*. 2021;26:100354. doi:10.1016/j.forc.2021.100354

56. Camurri G, Zaramella A. High-throughput liquid chromatography/mass spectrometry method for the determination of the chromatographic hydrophobicity index. *Anal Chem*. 2001;73(15): 3716-3722. doi:10.1021/ac001388j

57. Fuguet E, Ràfols C, Bosch E, Rosés M. Chromatographic hydrophobicity index: pH profile for polyprotic compounds. *J Chromatogr a*. 2009; 1216(45):7798-7805. doi:10.1016/j.chroma.2009.09.031

58. Valko K, Nunhuck S, Bevan C, Abraham MH, Reynolds DP. Fast gradient HPLC method to determine compounds binding to human serum albumin. Relationships with octanol/water and immobilized artificial membrane lipophilicity. *J Pharm Sci*. 2003;92(11):2236-2248. doi:10.1002/jps.10494

59. Valko K. Biomimetic chromatography to accelerate drug discovery: part 1. *LCGC Europe*. 2018;31(2):62-72.

60. Wang R, Fu Y, Lai L. A new atom-additive method for calculating partition coefficients. *J Chem Inf Comput*. 1997;37(3):615-621. doi:10.1021/ci960169p

61. Banker MJ, Clark TH, Williams JA. Development and validation of a 96-well equilibrium dialysis apparatus for measuring plasma protein binding. *J Pharm Sci*. 2003;92(5):967-974. doi:10.1002/jps.10332

62. Urien S, Albengres E, Comte A, Kiechel JR, Tillement JP. Plasma protein binding and erythrocyte partitioning of nicardipine in vitro. *J Cardiovasc Pharmacol*. 1985;7(5):891-898. doi:10.1097/00005344-198509000-00012

63. Manchester KR, Maskell PD, Waters L. Experimental versus theoretical log D7.4, pKa and plasma protein binding values for benzodiazepines appearing as new psychoactive substances. *Drug Test Anal*. 2018;10(8):1258-1269. doi:10.1002/dta.2387

64. Takács-Novák K. Physicochemical profiling in drug research and development. In: Mandic Z, ed. *Physico Chemical Methods in Drug Discovery and Development*. IAPC Publishing; 2012. doi:10.5599/obp.7.1

65. Wanka L, Iqbal K, Schreiner PR. The lipophilic bullet hits the targets: medicinal chemistry of adamantane derivatives. *Chem Rev*. 2013; 113(5):3516-3604. doi:10.1021/cr100264t

66. Kakehashi H, Shima N, Ishikawa A, et al. Effects of lipophilicity and functional groups of synthetic cannabinoids on their blood concentrations and urinary excretion. *Forensic Sci Int*. 2020;307:110106. doi:10.1016/j.forsciint.2019.110106

67. Lee KZH, Wang Z, Fong CY, Goh EML, Moy HY, Chan ECY. Identification of optimal urinary biomarkers of synthetic cannabinoids BZO-

HEXOXIZID, BZO-POXIZID, 5F-BZO-POXIZID, and BZO-CHMOXIZID for illicit abuse monitoring. *Clin Chem*. 2022;68(11): 1436-1448. doi:10.1093/clinchem/hvac138

68. Vikingsson S, Gréen H, Brinkhagen L, Mukhtar S, Josefsson M. Identification of AB-FUBINACA metabolites in authentic urine samples suitable as urinary markers of drug intake using liquid chromatography quadrupole tandem time of flight mass spectrometry. *Drug Test Anal*. 2016;8(9):950-956. doi:10.1002/dta.1896

69. Schaefer N, Kettner M, Laschke MW, et al. Distribution of synthetic cannabinoids JWH-210, RCS-4 and Δ 9-tetrahydrocannabinol after intravenous administration to pigs. *Curr Neuropharmacol*. 2017;15(5): 713-723. doi:10.2174/1570159X15666161111114214

70. Labiris NR, Dolovich MB. Pulmonary drug delivery. Part I: physiological factors affecting therapeutic effectiveness of aerosolized medications. *Br J Clin Pharmacol*. 2003;56(6):588-599. doi:10.1046/j.1365-2125.2003.01892.x

71. Schinkel AH. P-glycoprotein, a gatekeeper in the blood–brain barrier. *Adv Drug Deliv Rev*. 1999;36(2):179-194. doi:10.1016/S0169-409X(98)00085-4

72. Morales-Noé A, Esteve-Turrillas FA, Armenta S. Metabolism of third generation synthetic cannabinoids using zebrafish larvae. *Drug Test Anal*. 2022;14(4):594-603. doi:10.1002/dta.3195

73. Saito K, Kokaji Y, Muranaka Y, Ito R. Simultaneous determination of synthetic cannabinoids in illegal herbal products and blood by LC-TOF-MS, and linear regression analysis of retention time using log Pow. *Forensic Chem*. 2020;17:100202. doi:10.1016/j.forc.2019.100202

74. Hess C, Schoeder CT, Pillaiyar T, Madea B, Müller CE. Pharmacological evaluation of synthetic cannabinoids identified as constituents of spice. *Forensic Toxicol*. 2016;34(2):329-343. doi:10.1007/s11419-016-0320-2

75. Leibnitz S. Determination of the plasma protein binding of new psychoactive substances. Doctor of Medicine Dissertation. Saarland University; 2018. Accessed 8 September 2022. https://d-nb.info/1197054618/34

76. Miller RR, Madeira M, Wood HB, Geissler WM, Raab CE, Martin IJ. Integrating the impact of lipophilicity on potency and pharmacokinetic parameters enables the use of diverse chemical space during small molecule drug optimization. *J Med Chem*. 2020;63(21):12156-12170. doi:10.1021/acs.jmedchem.9b01813

77. Potts AJ, Cano C, Thomas SHL, Hill SL. Synthetic cannabinoid receptor agonists: classification and nomenclature. *Clin Toxicol*. 2020;58(2): 82-98. doi:10.1080/15563650.2019.1661425

SUPPORTING INFORMATION

Additional supporting information can be found online in the Supporting Information section at the end of this article.